ER : 1079
pp. 1–15 (col.fig.: NIL)
PROD. TYPE: COM
3B2
ED: UMA
PAGN: THILAKAM SCAN: ROOPA

INTERNATIONAL JOURNAL OF ENERGY RESEARCH
Int. J. Energy Res. 2004; **28**: 000–000
Published online in Wiley InterScience (www.interscience.wiley.com). DOI: 10.1002/er.1079

Parametric study of chemical looping combustion for tri-generation of hydrogen, heat, and electrical power with CO_2 capture

J. Wolf[1] and J. Yan[1,2,*,†]

[1] *Department of Chemical Engineering and Technology/Energy Processes, Royal Institute of Technology, Teknikringen 50, SE-10044 Stockholm, Sweden*
[2] *Department of Mechanical Engineering/Energy Engineering, Luleå University of Technology, SE-97187 Luleå, Sweden*

SUMMARY

In this article, a novel cycle configuration has been studied, termed the extended chemical looping combustion integrated in a steam-injected gas turbine cycle. The products of this system are hydrogen, heat, and electrical power. Furthermore, the system inherently separates the CO_2 and hydrogen that is produced during the combustion. The core process is an extended chemical looping combustion (exCLC) process which is based on classical chemical looping combustion (CLC). In classical CLC, a solid oxygen carrier circulates between two fluidized bed reactors and transports oxygen from the combustion air to the fuel; thus, the fuel is not mixed with air and an inherent CO_2 separation occurs. In exCLC the oxygen carrier circulates along with a carbon carrier between three fluidized bed reactors, one to oxidize the oxygen carrier, one to produces and separate the hydrogen, and one to regenerate the carbon carrier. The impacts of process parameters, such as flowrates and temperatures have been studied on the efficiencies of producing electrical power, hydrogen, and district heating and on the degree of capturing CO_2. The result shows that this process has the potential to achieve a thermal efficiency of 54% while 96% of the CO_2 is captured and compressed to 110 bar. Copyright © 2004 John Wiley & Sons, Ltd.

KEY WORDS: chemical looping combustion; CO_2 capture; hydrogen production; tri-generation; co-generation; STIG; parametric analysis; advanced power generation

1. INTRODUCTION

Climate change mitigation technologies (e.g. CO_2 capture) and hydrogen as energy carrier will play an increasing role in the future sustainable energy systems. For this reason, a process that cogenerates hydrogen and power and inherently captures CO_2 will be an interesting future energy conversion process. This process may have the potential to save investment and

*Correspondence to: J. Yan, Department of Mechanical Engineering/Energy Engineering, Luleå University of Technology, SE-97187 Luleå, Sweden.
†E-mail: yanjy@ket.kth.se

Contract/grant sponsor: Swedish Energy Agency (Energimyndigheten)

Received 9 June 2004
Accepted 3 September 2004

operating costs, because such a highly integrated plant will need less equipment than two separate plants and no fees for CO_2 emissions will have to be paid.

The core process of the system is an extended chemical looping combustion (exCLC) process, which is based on the classic chemical looping combustion (CLC) process. CLC represents an innovative way of capturing CO_2 in a power generation process. Pure CO_2 is obtained by applying a two-step combustion with inherent CO_2 separation. A solid oxygen carrier circulates between two fluidized bed reactors and transports oxygen from the combustion air to the fuel; thus, the fuel is not mixed with air and a subsequent CO_2 separation process is not necessary (more details in Section 2). The principles of CLC were introduced in the early 1980s (Richter and Knoche, 1983; Ishida *et al*., 1987). Since 1983, studies have been performed on process integration (Ishida and Jin, 1994; Anheden, 1997; Copeland *et al*., 2000; Wolf *et al*., 2001, 2004; Brandvoll and Bolland, 2002; Naqvi and Bolland, 2004), selection and preparation of oxygen carriers (Copeland *et al*., 2002; Ishida *et al*., 1998, 2002; Cho *et al*., 2002, 2004; Ryu *et al*., 2002; Mattisson *et al*., 2001), and reactor design (Lyngfelt *et al*., 2001; Johansson, 2002; Johansson *et al*., 2002; Kronberger *et al*., 2004; Adánez *et al*., 2003). When studying CLC, we found that by reducing the flowrate of oxygen carrier to under stoichiometric conditions in the fuel reactor it is possible to produce hydrogen as a by-product of the generation of electrical power. A pre-study of the required reactor conditions has been conducted by Hicking (2002) and in order to separate the hydrogen from the CO_2 in an efficient way, Wolf and Yan (2004) suggested the exCLC, where CO_2 and hydrogen is inherently separated; thus no external energy is needed for their purification.

In this paper, a novel cycle configuration is studied which we call the extended chemical looping combustion integrated in a steam-injected gas turbine cycle (exCLC-STIG). A steam-injected gas turbine cycle (STIG) is an advanced gas turbine cycle that augments the expander flow rate with steam generated through cycle heat recovery. Because the system is highly integrated, it is important to study the parameters on how them affect the performance of the system. Key parameters of the process are identified, and their impacts on the efficiencies of producing electrical power, hydrogen and district heating are investigated. Furthermore, the achievable degree of CO_2 capture is studied. The aim of the paper is to present this advanced tri-generation process with CO_2 capture and to show its potentials.

2. PRINCIPLES OF THE EXTENDED CLC

In the classic CLC process (Figure 1(a)), the separation of CO_2 from the combustion product gases occurs during the combustion process, in which the direct contact of fuel and combustion air is avoided. A solid oxygen carrier performs the task of carrying the oxygen from the air to the fuel gas. This means that the combustion occurs in two separate reactors. In the extended CLC (Figure 1(b)), the oxygen carrier circulates along with a carbon carrier between three fluidized bed reactors. The carbon carrier is calcium oxide (CaO) and the oxygen carrier is nickel oxide (NiO). In this system, not only does the inherent separation of carbon dioxide takes place, but also the production and separation of hydrogen. The hydrogen is produced by using an under-stoichiometric amount of active nickel oxide in the fuel reactor; thus, partial oxidation of methane (reaction Equation (1)) and steam reforming (reaction Equation (2)) take place. From reaction Equation (1), it can be read that nickel oxide will be reduced to nickel. In order to separate the hydrogen from the CO_2, the carbon carrier (calcium oxide) is used. Due to the

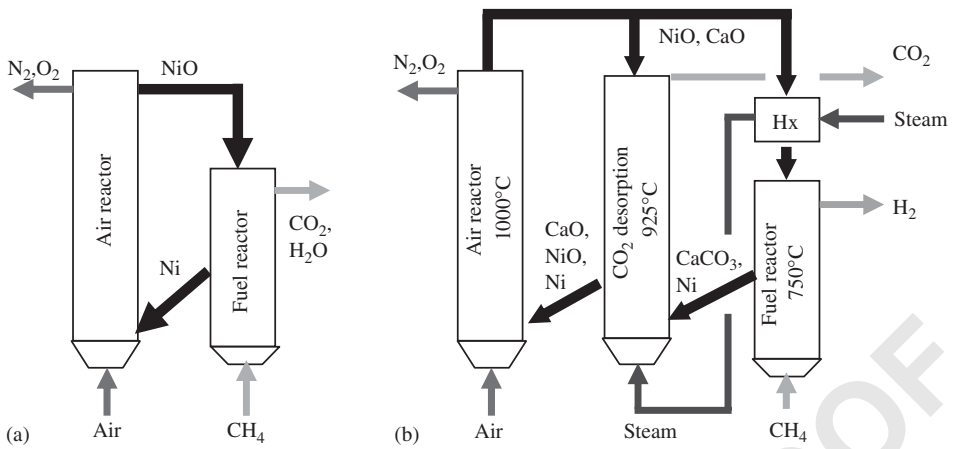

Figure 1. (a) Principles of the classic CLC, (b) principles of the exCLC.

presence of calcium oxide in the fuel reactor, the CO_2 will react to produce calcium carbonate ($CaCO_3$) according to reaction Equation (3). In this way, CO_2 is removed from the gaseous phase where only hydrogen and steam remain.

$$3NiO + CH_4 \rightarrow 3Ni + CO_2 + H_2O + H_2 \quad (1)$$

$$CH_4 + H_2O \rightarrow CO + 3H_2 \quad (2)$$

$$CaO + CO_2 \leftrightarrow CaCO_3 \quad (3)$$

$$CH_4 \rightarrow C + 2H_2 \quad (4)$$

$$C + H_2O \leftrightarrow CO + H_2 \quad (5)$$

$$CO + H_2O \leftrightarrow CO_2 + H_2 \quad (6)$$

However, if there is too little steam or oxygen available in the fuel reactor, the decomposition of methane will cause deposits of carbon on the particles of the carrier material (reaction Equation (4)). In order to avoid carbon deposits, it may be necessary to add steam to the fuel reactor such as in steam reforming (Twigg, 1989). In this way, the carbon will react to produce carbon monoxide according to the heterogeneous water–gas-shift reaction (reaction Equation (5)). Due to the homogeneous water–gas-shift reaction (reaction Equation (6)), the carbon monoxide will further react to CO_2 and, thereby, be removed from the gaseous phase when CO_2 reacts to calcium carbonate. These reactions are heavily dependent on temperature and control the composition of the gaseous phase. This gas composition has been studied at various temperatures in Wolf and Yan (2004).

In order to operate the fuel reactor at an appropriate temperature, the very hot particles that return from their regeneration have to be cooled. This is necessary for the formation of calcium carbonate. In Figure 1(b) it is shown how the combustion process may look like if steam is used to cool the particle stream before it enters the fuel reactor.

To regenerate the carbon carrier, the particles flow into a calcination reactor where calcium carbonate decomposes into calcium oxide and CO_2. In this reactor, the temperature must be above the decomposition temperature of calcium carbonate, i.e. the equilibrium of reaction (3) must be on the left-hand side. However, this calcination is endothermic and in order to maintain the required temperature it is necessary to supply additional heat. We suggest using a part-flow of the hot particle stream leaving the third reactor (the air reactor), in which the oxygen carrier is regenerated. However, depending on the temperature in the air reactor, the temperature obtained with this method may be too low for the calcination. Therefore, it will be necessary to reduce the partial pressure of CO_2 in the calcination reactor. For this reason, we introduce the hot steam that cooled the fuel reactor into the calcination reactor. The gaseous products of the calcination are CO_2 and steam. The oxygen carrier is inert in the calcination and has to be regenerated in the air reactor, where the reduced nickel oxide re-oxidizes according to reaction Equation (7).

$$Ni + 1/2O_2 \rightarrow NiO \quad \text{exothermic} \tag{7}$$

More details about the exCLC can be found in Wolf and Yan (2004)

3. SYSTEM CONFIGURATIONS

In STIG, the sensible heat of the turbine exhaust is used to generate steam that is then injected into the working fluid between the compressor and the expander (usually in the gas turbine combustor). This increases the flowrate through the turbine expander compared to the compressor such that the power output is increased. In this way, a STIG process needs no steam turbine and, therefore, has a simple design and the potential to lower investment costs. Moreover, the latent heat in the exhaust gas can be further recovered for district heating in a flue gas condenser. There are other cycle configurations that may improve the thermal efficiency of a power generation process with an exCLC, for example, a combined cycle or a humid air turbine cycle (Jonsson and Yan, 2004; Bartlett and Westermark, 2003). We chose the STIG cycle because of its potential to cogenerate the three products heat, hydrogen, and power by using a simple cycle configuration.

Figure 2 shows the flowchart of the whole exCLC-STIG process. The process starts with the turbine compressor that compresses the combustion air to 10 bar. The compressed air flows into the air reactor along with steam and oxygen carrier and carbon carrier particles. After the air reactor, the hot particles are separated from the gaseous phase and divided in two streams. The first stream flows directly into the calcination reactor where it supplies heat for the regeneration of the carbon carrier. The second stream is cooled by steam in a gas–solid heat exchanger (HX in Figure 2). This heat exchanger is designed as a fluidized bed and gives a high heat-exchange rate. The cooled and regenerated solids enter the fuel reactor in which hydrogen is produced. The particles then re-circulate for regeneration and hydrogen and steam exit the fuel reactor.

A part-flow of the hydrogen stream is used for top-firing in the gas turbine and the heat in the remaining product stream is recovered in the heat recovery steam generator (HRSG) (B1 in Figure 2). In the topping combustor, the hydrogen is combusted with excess oxygen from the air reactor. Thereafter, the hot gases pass through the gas-turbine expander and enter the HRSG (A1 and A2 in Figure 2). The hydrogen and the turbine exhausts are used to generate as much steam as possible and then district heating.

A third stream that leaves the exCLC is a mixture of steam and CO_2. This stream is mainly used to generate the steam that is needed to operate the calcination with low CO_2 partial

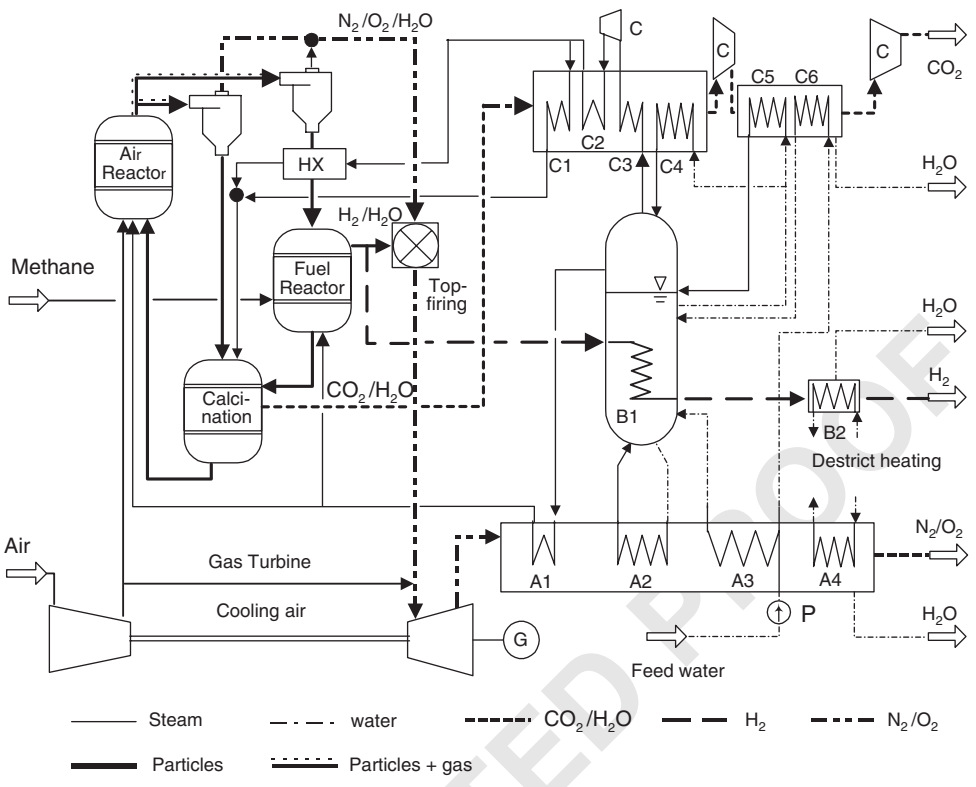

Figure 2. Flowsheet of the exCLC-STIG process.

pressure. In order to generate enough steam, it is necessary to compress the stream between evaporators C4 and C5 from 10 to 20 bar. In this way the dew point increases such that most of the steam can be condensed in the evaporator C5; thus, the heat of vaporization can be used to generate more steam. When all steam is removed from the CO_2 after heat exchanger C6, the CO_2 is compressed to 110 bar for final storage.

The products of this advanced power generation process with CO_2 capture are electrical power, compressed hydrogen, and district heating. Another feature of this cycle is that no external energy or equipment is required to separate CO_2 and hydrogen, which increases the performance of the process and may reduce the investment costs.

4. METHOD

In this paper, we have made a parameter study of the exCLC-STIG to investigate how the system's performance changes with the important parameters of the system. Five independent process parameters were identified which are f, T_{AR}, T_{TC}, R_{SM}, and z.

Parameter f determines the mass flowrate of particles that circulate between the air- and the calcination reactor in order to heat the calcination process. Here, f is the ratio of the particle stream that comes from the air reactor ($\dot{m}_{\mathrm{AR,out}}$) to the part-flow that enters the fuel reactor ($\dot{m}_{\mathrm{FR,in}}$).

$$f = \frac{\dot{m}_{\mathrm{AR,out}}}{\dot{m}_{\mathrm{FR,in}}} \tag{8}$$

$$\dot{m}_{\mathrm{CR,in}} = \dot{m}_{\mathrm{AR,out}} - \dot{m}_{\mathrm{FR,in}} \tag{9}$$

$$\dot{m}_{\mathrm{CR,in}} = (f - 1)\, \dot{m}_{\mathrm{FR,in}} \tag{10}$$

Because of Equations (9) and (10), this means the larger f is, the larger the flowrate of solids into the calcination reactor ($\dot{m}_{\mathrm{CR,in}}$) is.

T_{AR} is the temperature in the air reactor, T_{TC} is the temperature in the topping combustion, R_{SM} is the ratio of the mass flowrate of steam to fuel (methane) entering the fuel reactor, and z is the mass fraction of inactive material in the oxygen carrier particle.

The system's efficiencies are defined as the thermal efficiency (Equation (11)), the hydrogen efficiency (Equation (12)), the efficiency of electrical power (Equation (13)), the degree of CO_2 capture (Equation (14)), and the efficiency of district heating (Equation (15)).

$$\eta_{\mathrm{th}} = \frac{\dot{n}_{\mathrm{H_2,out}}\ \mathrm{LHV}_{\mathrm{H_2}} + P}{\dot{n}_{\mathrm{CH_4}}\ \mathrm{LHV}_{\mathrm{CH_4}}} \tag{11}$$

$$\eta_{\mathrm{H_2}} = \frac{\dot{n}_{\mathrm{H_2,out}}\ \mathrm{LHV}_{\mathrm{H_2}}}{\dot{n}_{\mathrm{CH_4}}\ \mathrm{LHV}_{\mathrm{CH_4}}} \tag{12}$$

$$\eta_{P} = \frac{P}{\dot{n}_{\mathrm{CH_4}}\ \mathrm{LHV}_{\mathrm{CH_4}}} \tag{13}$$

$$D_{\mathrm{CO_2}} = \frac{\dot{m}_{\mathrm{CO_2,captured}}}{\dot{m}_{\mathrm{CO_2,produced}}} \tag{14}$$

$$\eta_{\mathrm{DH}} = \frac{Q_{\mathrm{DH}}}{\dot{n}_{\mathrm{CH_4}}\ \mathrm{LHV}_{\mathrm{CH_4}}} \tag{15}$$

A model of the whole system was implemented in the simulation software Aspen Plus® and five series of simulations have been conducted, in which the five parameters were varied starting from a base case. In order to study the impact on the system of each parameters, we changed only one parameter during a series and kept the others as in the base case (if possible). The settings for the base case were $f = 8$, $T_{\mathrm{AR}} = 1000^{\circ}\mathrm{C}$, $T_{\mathrm{TC}} = 1150^{\circ}\mathrm{C}$, $R_{\mathrm{SM}} = 0.6$, $z = 0.4$. This base case was chosen, because it could be used over a wide range in the most of the series. However, it should be pointed out that in some cases, it was necessary to change two parameters in order to obtain the required T_{AR}.

Another important parameter has been studied. R_{SCa} is the ratio of the mass flowrate of steam to the mass flowrate of calcium carbonate into the calcination reactor. R_{SCa} controls the partial pressure of CO_2 in the calcinator. In contrast to the above defined parameters, R_{SCa} is not independent. On the contrary, T_{AR}, R_{SM}, and z influence the amount of steam passing the gas–solid heat exchanger (HX in Figure 2) and thereby they change R_{SCa}. This means that some of the impacts of the independent parameters on the system's performance, and here especially the

Table I. Assumption for the cycle calculations.

Efficiencies	
Isentropic efficiency of the gas turbine	90%
Isentropic efficiency of the compressor	85%
Isentropic efficiency of the booster fans	85%
Isentropic efficiency of the pumps	65%
Mechanical efficiency of the gas turbine	99%
Mechanical efficiency of the compressor	99%
Mechanical efficiency of the booster fans	99%
Mechanical efficiency of the pumps	99%
Efficiency of the generator	99%
Heat exchanger—min. temp. difference (°C)	
gas–gas heat exchanger	30
gas–water heat exchanger	10
water–water heat exchanger	10
Cooling of gas turbine	
Percentage of compressor air	11%
District heating	
Temperature of incoming water	50°C
Temperature of heated water	80°C
Low heating value (LHV)	
Methane ($kJ\,mol^{-1}$)	802
Hydrogen ($kJ\,mol^{-1}$)	242

CO_2 capture, are caused through changing R_{SCa}. Therefore, for a better understanding of the system, we also simulated a series, in which only R_{SCa} was varied while the other five parameters were kept as in the base case. In this simulation series, we added steam into the calcination reactor via heat exchanger C1 in Figure 2. In all other series, this stream was set to zero.

The assumptions for the performance analysis are summarized in Table I. One further assumption was that all calcium oxide reacts to calcium carbonate in the fuel reactor. In practice, a fraction of the particles will be inactive, as is the case with the oxygen carrier. However, the impact on the system's performance will be the same in both cases. For this reason, we included only the study of parameter z.

5. RESULTS AND DISCUSSION

The results from the parameter study are summarized in Sections 5.1–5.6 and Figure 3. All absolute figures in this section refer to an 800 MW_{th} exCLC, i.e. 1 kmol methane s^{-1} is used as feedstock. In Figure 3, the simulations where a second parameter was changed are marked with a yellow background. Section 5.7 contains an approach to optimize the system for the production of hydrogen and electrical power.

5.1. Impact of the steam to carbon carrier ratio in the calcination (R_{SCa})

Figure 3(a) shows the impact of the amount of steam that is injected into the calcination reactor in order to maintain a low CO_2 partial pressure during calcination. The diagram shows the

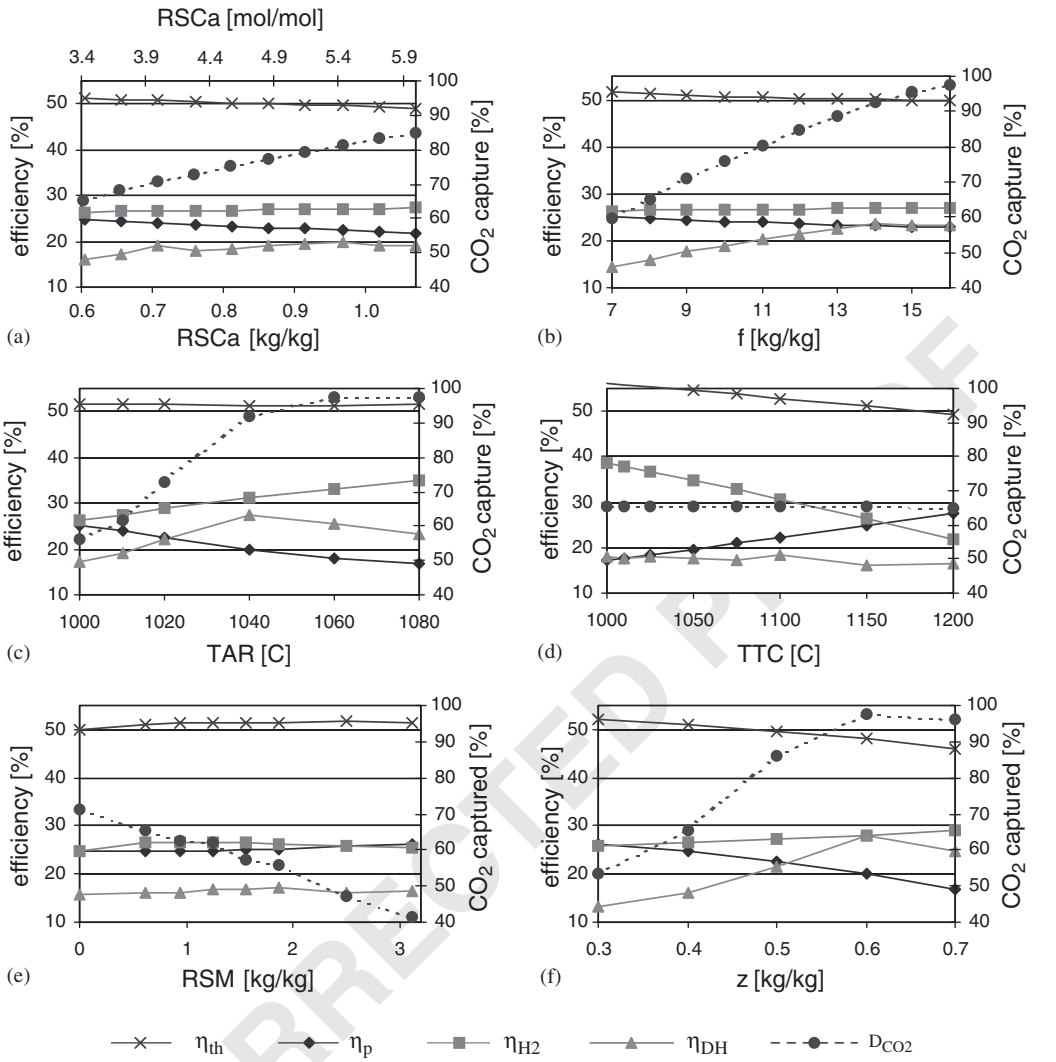

Figure 3. Results of the parameter study. The first y-axis shows the thermal efficiency (η_{th}), the power efficiency (η_P), the hydrogen efficiency (η_{H_2}), and the efficiency of district heating (η_{DH}). The y-axis on the right shows the degree of CO_2 capture (D_{CO_2}).

power-, hydrogen-, district heating-, and the thermal efficiency versus R_{SCa}. The y-axis on the right is the degree of capturing CO_2 in the process. One can see that the fraction of captured CO_2 increases when increasing R_{SCa}, although the temperature in the calcinator decreases from 938°C (when $R_{SCa} = 0.6$) down to 922°C ($R_{SCa} = 1.5$). This is because the steam that comes from heat exchanger C1 enters the calcinator at 700°C which cools the reactor. Figure 3 shows that the diluting effect of an increasing R_{SCa} has a stronger impact on the degree of CO_2 capture than its cooling effect.

When increasing R_{SCa}, the thermal efficiency decreases slightly, with an increase in η_{H_2} offsetting a decrease in η_P. This occurs because the more steam enters the calcination reactor, the more steam passes the vapour compression, which consumes some of the generated electrical power. This means the degree of CO_2 capture increases at the cost of power efficiency. The increase of the hydrogen efficiency occurs because less hydrogen is consumed in the topping combustion. The reason for this is a lower temperature of the oxygen- and carbon carrier after calcination when R_{SCa} is high. The lower temperature of the solid stream after calcination leads to a reduced combustion-air flow into the air reactor, because less air is required to cool the exothermic oxidation of the oxygen carrier. Therefore, less gas, which has to be heated by top-firing, will enter the topping combustion; thus, less hydrogen is needed in the topping combustion. The hydrogen that is saved increases the hydrogen efficiency slightly.

In the process, the waste heat in the hydrogen stream and the turbine exhaust are used for generating district heating. The efficiency of district heating in this case is about 18% and it is fairly constant over the studied range of R_{SCa}.

It can be concluded that increasing R_{SCa} is a very efficient way to improve the degree of CO_2 capture and it favours hydrogen production. However, if a high-power efficiency is desired, R_{SCa} should be kept as little as possible.

5.2. Impact of the amount of solids circulating between the air reactor and the calcination reactor (f)

In Figure 3(b), f is the independent variable which controls the flowrate of inert solids into the calcination reactor. The studied efficiencies are only little affected by increasing the rate of particle circulation between the air and the calcination reactor, except that the efficiency of district heating increases by 10 percentage points and that the degree of CO_2 capture increases from 60 to 96% over the studied range. The reason for this is the rising temperature in the calcination (T_{CR}) which increases from 924 to 955°C when f increases from 7 to 16. However, the disadvantage of increasing the efficiency of CO_2 capture by increasing the circulation rate is the increasing size of the air- and calcination reactor. For an 800 MW_{th} exCLC, the mass flowrate of the carrier materials into the calcination reactor will increase from 2300 to 5800 $kg\,s^{-1}$ over the studied range of f. Depending on the reactor construction, the feasible circulation rate will be limited. Moreover, more particles are necessary for operating the cycle, which will increase the costs. However, f is an effective parameter to control the temperature in the calcination reactor without affecting R_{SCa}.

5.3. Impact of the temperature in the air reactor

Figure 3(c) shows the impact of raising the temperature in the air reactor. The thermal efficiency is almost constant at 52% over a temperature range of 1000–1080°C. However, the degree of CO_2 capture increases from 55% at 1000°C to 96% at 1080°C. The strong impact of T_{AR} on the degree of CO_2 capture comes from the induced increase of both R_{SCa} and the T_{CR}, which is favourable for the regeneration of the carbon carrier. The diagram indicates that 96% of CO_2 capture is the maximum that can be achieved. The final 4% of CO_2 cannot be captured because the temperature in the fuel reactor (732°C) is too high to allow all CO_2 to be absorbed by the carbon carrier (Wolf and Yan, 2004). This means the produced hydrogen contains some CO_2, of which a part escapes from the process via the topping combustion.

Figure 3(c) shows another feature of the system. It is possible to optimize the process for hydrogen production or for power production. A lower temperature in the air reactor favours the power efficiency, because the gas flow through the cyclone and therewith through the turbine expander is larger. In this way, however, more hydrogen is consumed in the topping combustor, which decreases the hydrogen efficiency. If the temperature in the air reactor is higher, less hydrogen is required for top-firing and therefore more hydrogen can be saved in the process.

The figure also shows an increased production of district heating when the temperature in the air reactor is raised to 1040°C. This occurs as the oxygen factor in the air reactor is reduced because less heat has to be removed from the air reactor. The decreasing oxygen factor in the air reactor, however, is also a limiting parameter for the amount of steam that can be injected into this reactor. If the oxygen factor would fall below one, not all nickel will be re-oxidized leading to less oxygen transport, and the thermal capacity of the exCLC will be reduced. In order to extend the feasible temperature range, the steam injection into the air reactor can be decreased while more steam is injected into the fuel reactor. Therefore, the flowrate of steam into the fuel reactor was set to $30\,\mathrm{kg\,s^{-1}}$ in this simulation series instead of $10\,\mathrm{kg\,s^{-1}}$, as in the base case. If T_{AR} increases above 1040°C, η_{DH} decreases, because of an increased demand for steam in the gas–solid heat exchanger (HX in Figure 2). This means more heat is consumed in the economizer (A3 in Figure 2) which leaves less heat for district heating.

It can be concluded that increasing T_{AR} is an efficient way of improving CO_2 capture while retaining a high thermal efficiency. However, if electrical power is the desired product, then T_{AR} should be chosen as low as possible. Moreover, the material of the cyclones should be considered as the limiting factor for the temperature.

5.4. Effect of the temperature of the topping combustor

The temperature of the topping combustion is an effective parameter to shift the degree of efficiency between hydrogen and power production. Figure 3(d) shows that, starting from the base case, the hydrogen efficiency increases from ca. 25 to 40% when no top-firing is used. The hydrogen efficiency increases even more than the power efficiency decreases; thus, the combined hydrogen and power efficiency (η_{th}) increases from 52 to 54% when no top-firing is used. However, without top-firing the power efficiency will only be about 18%.

5.5. Effect of introducing steam to the fuel reactor

Injecting steam into the fuel reactor seems to have no positive effect on the cycle's efficiencies (Figure 3(e)). Moreover, the degree of CO_2 capture decreases from 70% if no steam is added into the fuel reactor ($R_{\mathrm{SM}} = 0$) to 40%, when R_{SM} is equal to three. The decrease of CO_2 capture is caused by a reduction of R_{SCa}. Due to the increased steam flow into the fuel reactor, less steam is required to cool the solids entering the fuel reactor. This reduces the R_{SCa} value in the calcination reactor, thus, the partial pressure of CO_2 in the calcination increases which leads to an incomplete regeneration of the carbon carrier.

Despite the negative effects of increasing R_{SM} on the efficiencies, it might be necessary to introduce some steam into the fuel reactor in order to avoid the formation of carbon on the particles. The conditions in the fuel reactor will be similar to the one in steam reforming where a R_{SM} of at least 1.7 is recommended (Twigg, 1989). This would lead to a CO_2 capture of only 55% which is not sufficient. Some of the other parameters have to be changed, for example, the temperature in the air reactor. From Figure 3(c), in which R_{SM} was equal to 1.9, it can be read

that a temperature in the air reactor of 1060°C would be sufficient to achieve the maximum possible CO_2 capture at a thermal efficiency of 52%.

5.6. Impact of the oxygen carrier's reactivity on cycle performance

If the particle reactivity decreases, the circulation rate of solids through the fuel reactor and the calcination reactor will increase. This has a positive impact on CO_2 capture and heat production. Since more steam is required in the HX to maintain 732°C in the fuel reactor, more steam enters the calcination reactor and R_{SCa} increases. A second reason is that T_{CR} increases because of the increased flowrate of solids from the air reactor. The increase of η_{DH} can be explained by reduction of the oxygen factor. Less air is required in the air reactor because of the larger amount of solids that has to be heated by the oxidation reaction. For z equal to 0.6 and 0.7, the oxygen factor will fall below one if the steam fraction in the air reactor is not decreased by increasing the steam flowrate into the fuel reactor. If z is larger than 0.7, more parameter have to be changed in order to achieve 1000°C in the air reactor, for example, reducing f. Nevertheless, this indicates that the inactive fraction of the oxygen carrier should be far below 0.7.

5.7. Optimization of the system

The results from Sections 5.1 to 5.6 can be used to optimize the tri-generation process for one of its main products and for CO_2 capture depending on the application of such systems. Table II shows the results of an optimization of the power and the hydrogen efficiency. The table shows the settings of the input parameters and the results of the efficiencies.

We optimized the η_P by increasing f to 12 and z to 0.5. T_{AR} and T_{TC} are kept constant from the base case. R_{SM} was set to 1.9 in order to avoid carbon deposits on the particles in the fuel reactor. The results show that a power efficiency of 24% can be achieved while the hydrogen efficiency is 23% and the degree of CO_2 capture is 95%. A further increase of the power efficiency could be possible by increasing the amount of active oxygen carrier in the fuel reactor (case η_P^* in Table II). However, even less hydrogen would be produced and the thermal efficiency (η_{th}) would fall below 40%.

When optimizing the process for hydrogen production, a high thermal efficiency of about 54% may be achieved. The hydrogen efficiency will be 40% while the power efficiency decreases to 14%. If hydrogen is the desired product, the topping combustion can be removed. In order to keep the degree of CO_2 capture above 95%, it is necessary to increase T_{AR} to 1040°C. These

Table II. Results of an optimization of the power and the hydrogen efficiency.

	Input parameter						Results of the efficiencies (%)				
Optimized efficiency	f	T_{AR}	T_{TC}	R_{SM}	R_{SCa}	z	η_P	η_{H_2}	η_{th}	η_{CO_2}	η_{DH}
η_P	12	1000	1200	1.9	0.67	0.5	24	23	47	95	27
η_{H_2}	10	1040	1040	1.9	0.64	0.4	14	40	54	96	25
η_P^*	10	1000	1200	1.9	0.9	0.4	34	3	37	96	54[†]

*The fraction of active oxygen carrier is increased such that less hydrogen is produced in the fuel reactor.
[†]The supply-temperature for district heating is reduced from 80 to 70°C.

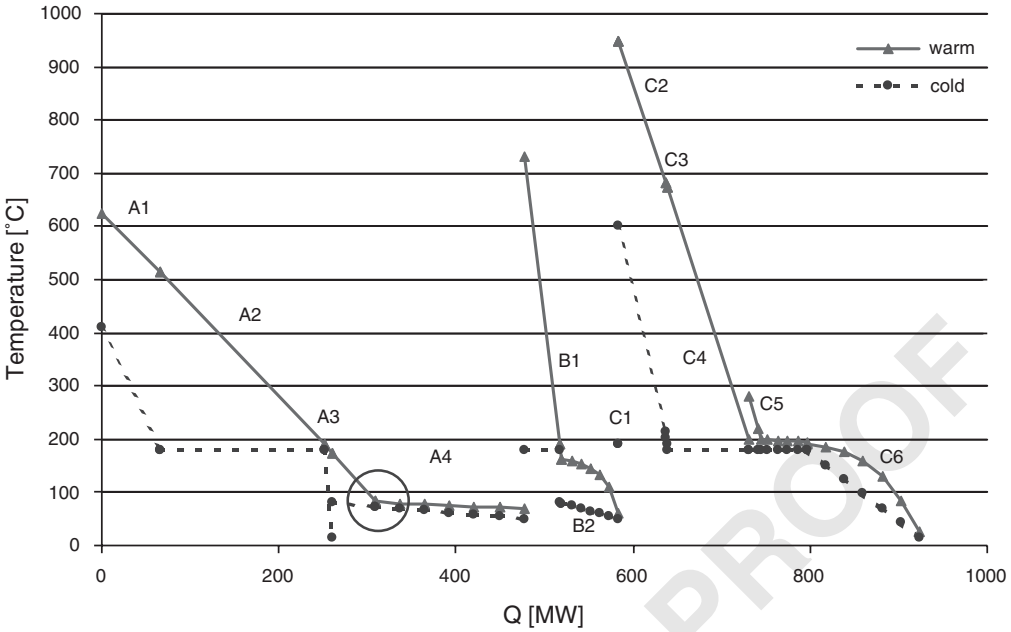

Figure 4. Results of the heat recovery if η_P is optimized. The heat exchanges A*i*, B*i*, and C*i* can be found in Figure 2.

settings are also an optimization for the thermal efficiency, given that a high degree of CO_2 capture is required and T_{AR} should be as low as possible in order to ease the reactor design.

From Table II one can read that the total efficiency of the system ($\eta_{th} + \eta_{DH}$) is about 75%, if the supply-temperature for the district-heating net is set to 80°C. The total efficiency can be improved by lowering the output temperature for the district heating from 80 to 70°C, for example. Figure 4 shows the temperature profile of the heat recovery with heat exchangers A4 and B2 for district heating. One can see that the output temperature of the exhaust gas after A4 is high enough to produce more district heating. The dew-point of the exhaust gas, however, is too low to produce more district heating at 80°C. Further calculations showed that at a supply-temperature of 70°C a total efficiency of over 90% is possible (case η_P^* in Table II).

6. CONCLUSION

Tri-generation of hydrogen, electrical power, and district heating has been studied in a novel process with CO_2 capture. The process is called the extended chemical looping combustion integrated in a steam-injected gas turbine cycle (exCLC-STIG). A parametric study showed the potential of the process and the following conclusions can be drawn:

- Cogeneration of hydrogen and power in this CO_2-free power generation process is theoretically possible. The results show that hydrogen production is a promising

application for chemical looping combustion, since a thermal efficiency of about 54% might be achieved.

- The process can be optimized for hydrogen production or power generation, depending on the application of the system. If a degree of CO_2 capture of at least 95% is desired, the power efficiency may reach 24%, when optimized for power efficiency. The maximum hydrogen efficiency may reach almost 40%, when optimized for hydrogen production. In the first case, the thermal efficiency will be about 47% and in the second case it will be about 54%.
- Hydrogen production gives the possibility to use top-firing to raise the turbine inlet temperature without loosing a high efficiency of CO_2 capture. In this way, very high temperatures above 1000°C in the exCLC can be avoided.
- Experiments are required to confirm the results of this paper and to determine the fraction of active material in the carbon carrier and the oxygen carrier. It may be necessary to develop special particles for both oxygen carrier and carbon carrier for the application in the exCLC.
- The reactor for the exCLC will be more complicated than that for the classic CLC. More research is required to find a suitable reactor design.
- It has to be investigated if it is necessary to install a fuel gas cleaning before the natural gas enters the exCLC in order to protect the oxygen- and carbon carrier from sulphur and sulphur components.

NOMENCLATURE

CLC = chemical looping combustion
exCLC = extended chemical looping combustion
f = ratio of mass flowrate of particles out of the air reactor to the part-flow of particles into the fuel reactor ($kg\,kg^{-1}$) (Equation (8))
$\dot{m}$ = mass flowrate ($kg\,s^{-1}$)
$\dot{n}_{CH_4}$ = the mole flow of methane, that is combusted in the process
$\dot{n}_{H_2,out}$ = the mole flow of hydrogen that is for sale
NGCC = natural gas fired combined cycle
P = power output
Q_{DH} = thermal energy for district heating
R_{SCa} = ratio of mass flowrate of steam to $CaCO_3$ in the calcination ($kg\,kg^{-1}$)
R_{SM} = ratio of mass flowrate of steam to methane ($kg\,kg^{-1}$)
STIG = steam-injected gas turbine
T_{AR} = temperature in the air reactor (°C)
T_{CR} = temperature in the calcination (°C)
T_{TC} = temperature in the topping combustion (°C)
z = mass fraction of inactive material in the oxygen carrier

Greek letters

η_{CO_2} = efficiency of CO_2 capture (Equation (14))
η_{DH} = efficiency of district heating (Equation (15))

η_{H_2} = hydrogen efficiency (Equation (12))
η_P = electrical power efficiency (Equation (13))
η_{th} = thermal efficiency, also called combined hydrogen and electrical power efficiency (Equation (11))

ACKNOWLEDGEMENT

Financial support from the Swedish Energy Agency (Energimyndigheten) is gratefully acknowledged.

REFERENCES

Adánez J, Garcia-Labiano F, de Diego LF, Plata A, Celaya J, Gayán P, Abad A. 2003. Opimizing the fuel reactor for chemical-looping combustion. *Proceedings of FBC2003, 17th International Fluidized Bed Combustion Conference*. Jacksonville, FL, U.S.A., 18–21 May.

Anheden M. 1997. Analysis of chemical-looping combustion systems for power generation. *Technical Licentiate Thesis*, Royal Institute of Technology, Department of Chemical Engineering and Technology, Energy Processes. Stockholm, ISSN 1104-3466, ISRN KTH/KET/R-62-SE.

Bartlett MA, Westermark MO. 2003. A study of humidified for short-term realisation gas turbines in mid-size power generation. *Proceedings of TURBO EXPO 2003*. Atlanta, U.S.A., Paper No. GT 2003-38402.

Brandvoll Ø, Bolland O. 2002. Inherent CO_2 capture using chemical looping combustion in a natural gas fired power cycle. *Proceedings of ASME TURBO EXPO 2002*: *Land*, *Sea*, *and Air*, Amsterdam, The Netherlands.

Cho P, Mattisson T, Lyngfelt A. 2002. Reactivity of iron oxide with methane in a laboratory fluidized bed—application of chemical looping combustion. *Proceedings of the 7th International Conference on Fluidized Bed Combustion*. Niagara Falls, Canada, 599.

Cho P, Mattisson T, Lyngfelt A. 2004. Comparison of iron-, nickel-, copper- and manganese-based oxygen carriers for chemical-looping combustion. *Fuel*, submitted for publication.

Copeland RJ, Alptekin G, Cesario M, Gebhard S, Gershanovich Y. 2000. A novel CO_2 separation system. *Proceedings of the 8th International Symposium on Transport and Dynamics of Rotating Machinery* (*ISROMAC-8*), Honolulu, Hawaii.

Copeland RJ, Alptekin G, Cesario M, Gershanovich Y. 2002. Sorbent energy transfer system (SETS) for CO_2 separation with high efficiency. *Proceedings of the 27th International Technical Conference on Coal Utilization & Fuel Systems*, Clearwater, FL, U.S.A.

Hicking B. 2002. Simulation of chemical-looping combustion for CO_2 separation in power generation processes. *Master of Science Thesis*, Department of Chemical Engineering and Technology, Energy Processes, Royal Institute of Technology, Stockholm, Sweden.

Ishida M, Jin H. 1994. A new advanced power-generation system using chemical-looping combustion. *Energy* **19**(4):415.

Ishida M, Jin H, Akehata T. 1987. Evaluation of a chemical-looping-combustion power-generation system by graphic exergy analysis. *Energy* **12**(2):147.

Ishida M, Jin H, Okamoto. 1998. Kinetic behavior of solid particle in chemical-looping combustion: suppressing carbon deposition in reduction. *Energy & Fuels* **12**:223.

Ishida M, Yamamoto M, Ohba T. 2002. Experimental results of chemical-looping combustion with $NiO/NiAl_2O_4$ particle circulation at 1200°C. *Energy Conversion and Management* **43**:1469.

Johansson E. 2002. Interconnected fluidized bed for chemical-looping combustion with inherent CO_2-seperation. *Technical Licentiate Thesis*, Department of Energy Conversion, Chalmers University of Technology, Gothenborg, Sweden, ISSN 0281-0034.

Johansson E, Lyngfelt A, Mattisson T, Johnsson F. 2002. A circulating fluidized bed combustor system with inherent CO_2 separation—application of chemical looping combustion. *Proceedings of the 7th International Conference on Fluidized Bed Combustion*, Niagara Falls, Canada 717.

Jonsson M, Yan J. 2004. Humidified gas turbine—a review of proposed and implemented cycles. *Energy*, Manuscript.

Kronberger B, Löffler G, Hofbauer H. 2004. Simulation of mass and energy balances of a chemical-looping combustion system. *International Journal on Energy for a Clean Environment*, submitted for publication.

Lyngfelt A, Leckner B, Mattisson T. 2001. A fluidized-bed combustion process with inherent CO_2 separation; application of chemical-looping combustion. *Chemical Engineering Science* **56**:3101.

Mattisson T, Lyngfelt A,Cho P. 2001. The use of iron oxide as an oxygen carrier in chemical-looping combustion of methane with inherent separation of CO_2. *Fuel* **80**:1953.

Naqvi R, Bolland O. 2004. Chemical looping combustion analysis of natural gas fired power cycles with inherent CO_2 capture. *Proceedings of ASME TURBO EXPO 2004*: *Land*, *Sea*, *and Air*, Vienna, Austria, 14–17 June.

Richter HJ, Knoche KF. 1983. Reversibility of combustion processes, efficiency and costing. In *Second Law Analysis of Processes*, Gaggioli RA (ed.), ACS Symposium Series, vol. 235. Washington, DC, 71–85.

Ryu H-J, Bae D-H, Jin G-T. 2002. Carbon deposition characteristics of NiO based oxygen carriers particles for chemical-looping combustion. *6th International Conference on Greenhouse Gas Control Technologies*, Kyoto, Japan.

Twigg MV. 1989. *Catalyst Handbook* (2nd edn). Wolfe Publishing Ltd, ISBN 0-7234-0857-2.

Wolf J, Anheden M, Yan J. 2001. Performance analysis of combined cycles with chemical looping combustion for CO_2 capture. *Proceedings of the International Pittsburgh Coal Conference*, Newcastle, NSW, Australia.

Wolf J, Anheden M, Yan J. 2004. Comparison of nickel- and iron-based oxygen carriers in chemical looping combustion for CO_2 capture in power generation. *Fuel*, submitted for publication.

Wolf J, Yan J. 2004. Cogeneration of hydrogen and electrical power in an extended chemical-looping combustion. *Proceedings of ECOS 2004*, Guanajuato, Mexico, 7–9 July.

